Archives of Biochemistry and Biophysics 507 (2011) 44–55

Contents lists available at ScienceDirect

Archives of Biochemistry and Biophysics

journal homepage: www.elsevier.com/locate/yabbi

Review

Spectroscopic characterization of cytochrome P450 Compound I

Christiane Jung [a,*], Simon de Vries [b], Volker Schünemann [c,*]

[a] Max-Delbrück-Center for Molecular Medicine, Robert-Rössle Strasse 10, 13125 Berlin, Germany
[b] Laboratory of Biotechnology, Delft University of Technology, Julianalaan 67, 2628 BC Delft, The Netherlands
[c] Dept. of Physics, University Kaiserslautern, Erwin-Schrödinger-Strasse 46, 67663 Kaiserslautern, Germany

ARTICLE INFO

Article history:
Available online 30 December 2010

Keywords:
Cytochrome P450
Compound I
Iron-oxo species
Spectroscopy

ABSTRACT

The cytochrome P450 protein-bound porphyrin complex with the iron-coordinated active oxygen atom as Fe(IV)=O is called Compound I (Cpd I). Cpd I is the intermediate species proposed to hydroxylate directly the inert carbon–hydrogen bonds of P450 substrates. In the natural reaction cycle of cytochrome P450 Cpd I has not yet been detected, presumably because it is very short-lived. A great variety of experimental approaches has been applied to produce Cpd I artificially aiming to characterize its electronic structure with spectroscopic techniques. In spite of these attempts, none of the spectroscopic studies of the last decades proved capable of univocally identifying the electronic state of P450 Cpd I. Very recently, however, Rittle and Green [9] have shown that Cpd I of CYP119, the thermophillic P450 from *Sulfolobus acidocaldarius*, is univocally a Fe(IV)=O–porphyrin radical with the ferryl iron spin ($S = 1$) antiferromagnetically coupled to the porphyrin radical spin ($S' = 1/2$) yielding a $S_{tot} = 1/2$ ground state very similar to Cpd I of chloroperoxidase from *Caldariomyces fumago*. In this mini-review the efforts to characterize Cpd I of cytochrome P450 by spectroscopic methods are summarized.

Introduction

The name cytochrome P450 (P450)[1] stays for a large number of enzymes found in different organisms such as bacteria, fungi, mammals, and humans which catalyze the conversion of a variety of chemically diverse compounds [1]. Cytochromes P450 are heme thiolate proteins and members of the so-called CYP-superfamily currently consisting of 12,476 already named P450s. Bioinformatic analyses suggest the existence of approximately 6000 additional members, which have not yet been named [2].

In cytochrome P450s, the heme is bound to the protein matrix by coordination of the H-bonded, negatively charged sulfur atom of a cysteine to the iron, by salt links, by several van der Waals contacts and by H-bonded water molecules present in the heme pocket [3] (Fig. 1).

The main steps in the P450 reaction cycle (Fig. 2) include (i) substrate (–C–H) binding to the Fe^{3+} form of P450 accompanied by a spin state change from low-spin to high-spin in most of the enzymes; (ii) first reduction to build up the Fe^{2+} state; (iii) binding of O_2 to the Fe^{2+} heme, (iv) delivery of the second electron; (v) cleavage of the O–O bond of the iron bound dioxygen; (vi) insertion of an oxygen atom into the substrate; and (vii) release of the hydroxylated product (–C–OH). Along the Step (v) an intermediate heme iron-bound oxygen species is formed that is called "Compound I" (Cpd I) and believed to represent the active species, which directly hydroxylates the substrates [4]. There has been a general consensus in the P450 community that Cpd I, resulting from the heterolytic splitting of the O–O bond, does really exist and represents an iron-oxo species with iron in the Fe(IV) state and the porphyrin with the cation radical in the π-system [5–8]. The addition of one electron to Cpd I results in the formation of a species which is called Compound II (Cpd II).

The way to prove this Cpd I hypothesis is to compare the spectroscopic properties and parameters of this presumed Cpd I species with well-studied reference samples for which the spectroscopic assignment to Fe(IV) and the porphyrin-π-cation radical has been unambiguously demonstrated. Although a number of experimental and theoretical studies have been performed in the last 45 years, the electronic structure of P450 Cpd I has not been finally characterized because this intermediate is very short-lived and difficult

* Corresponding authors. Present address: KKS Ultraschall AG, Medical Surface Center, Frauholzring 29, CH-6422 Steinen, SZ, Switzerland. Fax: +41 41 8104508 (C. Jung).

E-mail addresses: christiane_jung@bluewin.ch, christiane_jung@hotmail.com, cjung@mdc-berlin.de (C. Jung), schuene@physik.uni-kl.de (V. Schünemann).

[1] *Abbreviations used:* P450cam, cytochrome P450cam from *Pseudomonas putida*, CYP101; Pdx, putidaredoxin; BMP, the heme protein domain of the monooxygenase P450BM-3 from *Bacillus megaterium*, CYP102; HRP, horseradish peroxidase; CPO, chloroperoxidase from *Caldariomyces fumago*; NADP(H), nicotinamide adenine (di)nucleotide phosphate, reduced form; m-CPBA, meta-chloroperoxybenzoic acid; PA, peroxy acetic acid; EPR, electron spin paramagnetic resonance; EXAFS, extended X-ray absorption fine structure; ENDOR, electron-nuclear double resonance; DFT, density functional theory; NIS, nuclear inelastic scattering; IR, infrared; RR, resonance Raman; NOS, nitric oxide synthase; iNOSox, inducible NOS oxygen domain; nNOSox, neuronal NOS oxygen domain.

0003-9861/$ - see front matter © 2010 Elsevier Inc. All rights reserved.
doi:10.1016/j.abb.2010.12.029

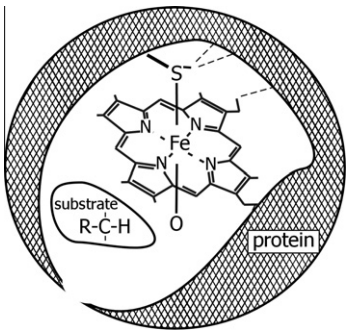

Fig. 1. Sketch of the structure of Compound I in cytochrome P450.

to trap experimentally. Just recently, however, Rittle and Green [9] were able to generate Cpd I of the thermostable CYP119 from *Sulfolobus acidocaldarius* in high yields using the shunt pathway displayed in Fig. 2 with *m*-CPBA as oxidant.

This article summarizes key spectroscopic studies, which have pursued the characterization of Cpd I in P450. In order to understand and judge the outcome of these studies a short background of the spectroscopic methods used and the specific application to heme proteins will be included. Because the presumed Cpd I in P450 is very short-lived the approaches and techniques used to catch this intermediate must also be discussed. A special emphasis is given to discuss the experimental conditions under which the trapped species are characterized. This should help in understanding the controversial nature of the observations made for the P450 intermediate.

Overview of the spectroscopic methods relevant for characterization of Compound I

The porphyrin chromophor of heme proteins enables the application of a great variety of spectroscopic techniques to determine its electronic structure and derived chemical structure (Fig. 3).

The biological models for Cpd I of P450 are peroxidases [10–12] while the non-biological models are the porphyrin iron complexes. Both these models have been extensively characterized with the techniques shown in Fig. 3. Not all of these techniques have or can be used for characterization of the presumed Cpd I of P450. The following spectroscopic methods that are relevant to the study of Cpd I P450 intermediates in comparison to models (peroxidases, porphyrin complexes) will be discussed (i) UV–visible electronic absorption spectroscopy (UV–vis); (ii) electron paramagnetic spectroscopy (EPR); (iii) Mössbauer spectroscopy; (iv) vibrational spectroscopy (resonance Raman (RR), infrared (IR), nuclear inelastic scattering (NIS)); (v) extended X-ray absorption fine structure spectroscopy (EXAFS); and (vi) X-ray crystallography.

The following experimental techniques for trapping reaction intermediates like Cpd I have been used in the past decades: (i) stopped-flow approach with rapid-scanning UV–vis detection; (ii) rapid-mixing freeze–quench approach (RFQ); (iii) radiation techniques; and (iv) photolysis (Fig. 4). Each of the methods mentioned above has its special requirements such as, for example, the specific state of the sample, and perhaps most importantly the detection limits, particularly important for experiments on short-lived reaction intermediates. Therefore we will first discuss in Trapping methods section how these techniques work and what their sample requirements are.

Trapping methods

Stopped-flow approach with rapid-scanning UV–vis detection

The stopped-flow approach is a technique which is most often used for the characterization of short-lived intermediates in solution. The simplest experimental set-up consists of two syringes, one filled with enzyme solution and the other with substrate or, for the study of the shunt reaction (Fig. 2), with oxidants like H_2O_2, peroxyacetic acid (PA) or *meta*-chloroperoxybenzoic acid (*m*-CPBA) (Fig. 4a). The plungers of the syringes are driven by pressured air and a T-mixer or Berger ball mixer mixes the liquids coming from the syringes with a time resolution of approximately 1 ms. The mixer unit is connected to an optical cell with a volume of approximately 20 μl consisting of quartz, which is transparent to light. In order to acquire UV–vis spectra of reasonable signal to noise ratio normally an optical path of 10 mm and enzyme concentrations of, e.g., P450cam in the range of 5–20 μM are required. After the experiment the reaction mixture is dumped and lost for further investigations. For this technique sample volumes in the milliliter range are required and the shortest time that can be achieved with standard commercial set-ups is approximately 1–2 ms.

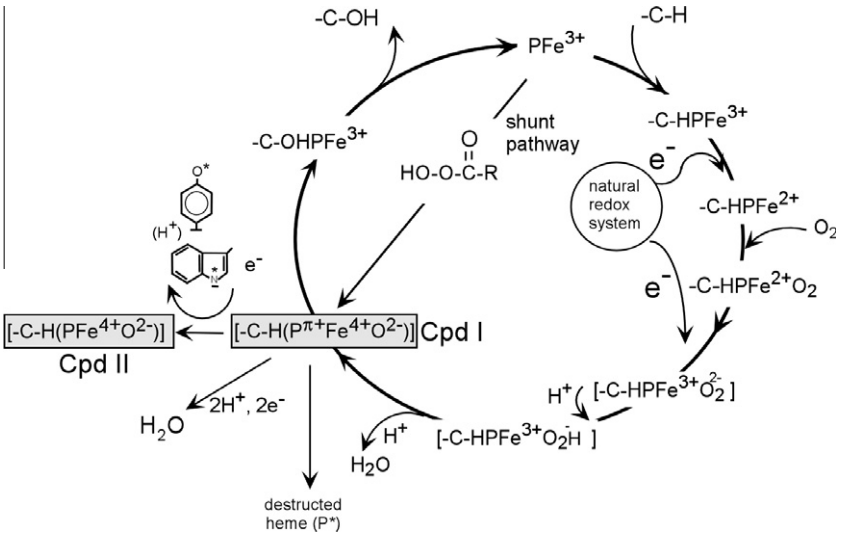

Fig. 2. Reaction cycle of cytochrome P450.

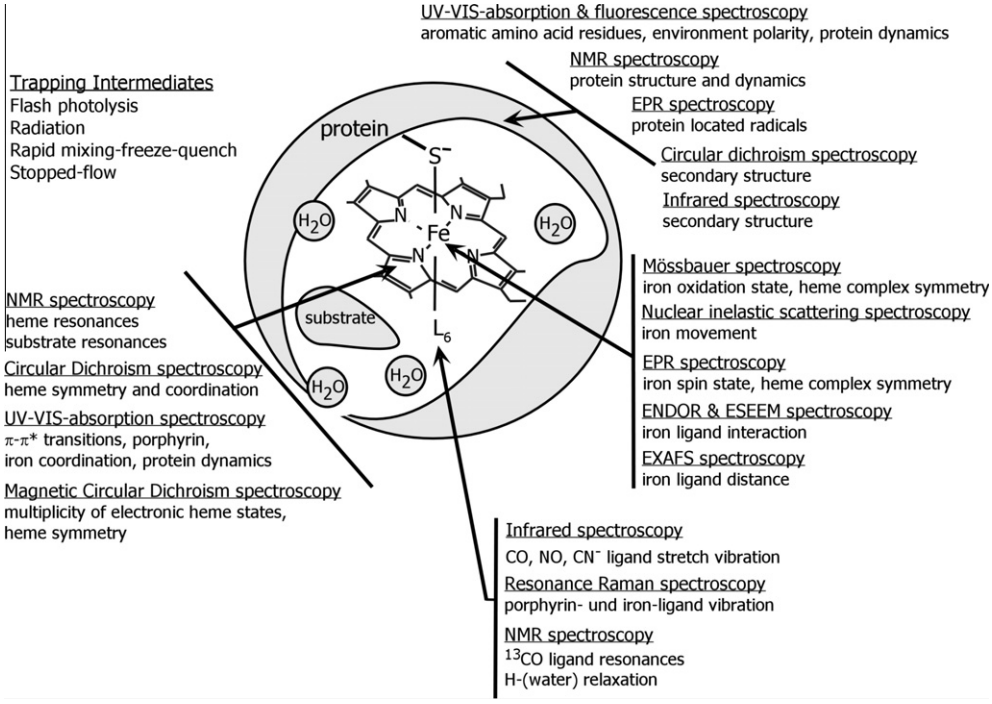

Fig. 3. Chromophors and spectroscopic techniques used to characterize structural and electronic properties of heme proteins.

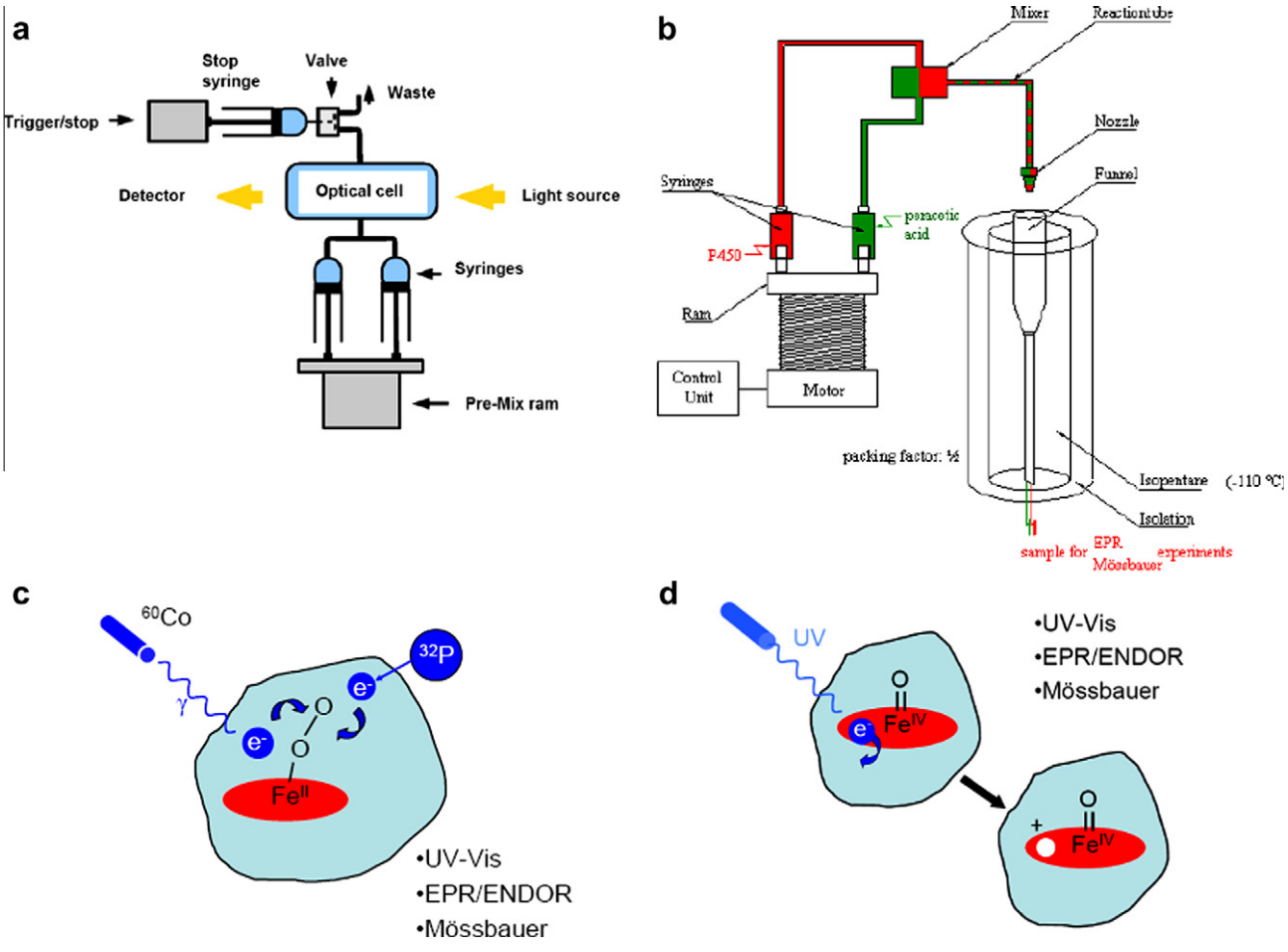

Fig. 4. Schematic pictures of the trapping techniques stopped-flow-approach (a), rapid freeze–quench (b), radiation techniques (c), and photolysis (d).

Rapid-mixing freeze–quench approach

This technique which is also denoted as rapid freeze–quench (RFQ) is used to cryo-trap solutions of reaction mixtures and yields frozen samples which can be investigated by spectroscopic methods like EPR, EXAFS, Mössbauer spectroscopy, and NIS as well as resonance Raman spectroscopy (Fig. 4b). For a typical trapping experiment using the shunt mechanism again two syringes are filled with enzyme and oxidant. The syringes are either driven with a mechanical hub or with pressurized air depending on the manufacturer of the system. In the RFQ systems developed by Ballou and Palmer [13] the solutions are mixed in a four-jet tangential mixer and travel through a reaction tube the length of which determines the reaction time of the solution. With the Model 1019 Syringe Ram manufactured by Update Instrument Inc. modified after the instrument developed by Ballou and Palmer the shortest reaction times of 5–7 ms can be reached with special tubes of 1 cm length [13,14]. The reaction mixture leaves the tube through a fine nozzle and is sprayed into a cold isopentane bath which can be kept liquid down to temperatures of approximately 130–140 K. After the freezing process the frozen powder is collected from the bath and packed into sample holders specific for the spectroscopic method used. The packing process of the samples has to be performed at the temperature of the isopentane bath in order to avoid further reaction of the trapped intermediates. This method requires a sample volume of typically 1 ml with the absolute lower limit being 300 μl. The shortest reaction time of a standard RFQ-experiment is determined by the freezing time and the time needed for the travel of the droplets from the nozzle into the liquid isopentane bath. This time is in the order of 5–7 ms depending on the type of set-up and can be determined by calibration with reactions of known kinetics (like, e.g., the reaction of myoglobin with azide) [14]. It is also possible to reach reaction times in the μs-range by using ultrafast mixing experiments in vacuum and subsequent freezing on cold metal surfaces [15,16], but these techniques have not been applied to trap Cpd I of P450s so far.

Radiation techniques

In the course of the reaction cycle for generation of Cpd I electrons must be supplied to the heme. Photoinduced injection of electrons to ferric P450 by illuminating the protein with light of a wavelength lower than 320 nm has been reported already in the nineteen eighties [17,18]. X-ray photoinduced production of electrons has also been applied on the dioxygen complex of P450cam to inject the so-called second electron. Nyman and Debrunner [19] as well as Hüttermann and coworkers [20] were the first to study the reaction by reducing P450cam–O_2 with X-rays at 80 K. The Hoffman group employed γ-irradiation at cryogenic temperatures of the ternary complexes of camphor, dioxygen, and ferro-cytochrome P450cam to inject the "second" electron of the catalytic process and were able to detect hydroxy-camphor as product which means that an oxidizing intermediate species has been formed [21]. The intermediate oxidizing species could however not been trapped and characterized. The β-radiation of radioactive ^{32}P may serve as an alternative radiation source to γ-rays [22] (Fig. 4c).

Photolysis approach

As an alternative to the oxidation of the ferric state of hemes and porphyrins the photochemical oxidation of Cpd II to Cpd I species has been investigated in enzymes and in models [23,24]. This approach requires that one can trap Cpd II species cleanly and in high yields before the laser flash photolysis (LFP) used for photooxidation is applied (Fig. 4d).

The preparation of Cpd II species in high yields can in principle be achieved by the reaction with excess peroxynitrite in a stopped-flow mixing apparatus. Once the UV–vis spectrum of the reaction mixture is similar to that expected for a pure Cpd II intermediate, UV-irradiation is applied in order to photooxidize Cpd II to Cpd I. This procedure was performed on a number of CYPs, i.e., the thermostable cytochrome P450 from *Sulfolobus solfactaricus* (CYP119) by the Newcomb group [24]. They used enzyme concentrations of 10–20 μM and irradiated the reaction mixture inside the stopped-flow cell with the 355 nm light (typically 5 mJ) from a pulsed Nd:YAG laser.

Spectroscopic methods

UV–visible electronic absorption spectroscopy

This spectroscopic technique measures the electronic transitions of the heme complex. The intense Soret (B) band between 370 and 450 nm and the significantly weaker α and β (Q) bands between 530 and 600 nm originate from the same π–π*-transitions of the porphyrin (a_{1u},$a_{2u} \rightarrow e_g^*$) which couple with porphyrin vibrational transitions and charge-transfer transitions between the porphyrin and the axial orbital system. In particular this latter coupling is the physical basis as to why the spectra of different heme proteins or heme complexes show some features such as the shift of the Soret band or the appearance of additional weak long-wavelength bands that may be used for identification of structural properties. In addition, formation of a π-cation radical of the porphyrin itself results in a long-wavelength band in the range of 680–800 nm. However, in contrast to other chromophors the porphyrin is a "soft" chromophor meaning that the position of the Soret band alone is not sufficient to unambiguously identify the structure of the heme complex. It is important to observe both the Soret band shift and the appearance of additional bands when P450 complexes are compared with model heme complexes.

The reaction of chloroperoxidase (CPO) with oxidants like H_2O_2, PA or *m*-CPBA has been taken as a model for the so called shunt pathway in P450 and nitric oxide synthase (NOS) since it follows the direct pathway from peroxide binding to the formation of the iron-oxo species which produces the hydroxylating intermediate. When CPO is mixed in stopped-flow experiments with an oxidant such as H_2O_2, PA or *m*-CPBA a green-colored Cpd I species is formed. CPO Cpd I shows an UV–vis absorption spectrum characterized by a broad Soret band around 370 nm and a weak, but significant long-wavelength band at ~690 nm [25,26] (Fig. 5). This spectrum is characteristic for a porphyrin-π-cation radical, very well known from iron porphyrin model complexes [27,28].

Stopped-flow experiments with oxidants similar to that described above for CPO have been performed on P450cam (CYP101) [29] and on the thermostable CYP119 [30]. The shortest time for UV–vis detection of CYP101 and CYP119 by using *m*-CPBA as oxidant was 6 ms and 2 ms, respectively. In contrast to CPO, the spectrum of an intermediate is only resolved after treatment of a set of spectra at different time points using the singular value decomposition method. It turned out that one singular value component, representing only 2–3% of the spectral changes, shows a spectrum which resembles that observed for CPO. This result has been taken as proof that a porphyrin-π-cation radical is formed also in P450. On the other hand in earlier studies, Pederson et al. [31], Wagner et al. [32], and Sligar et al. [33] reported optical spectra of an intermediate in the reaction of P450cam with PA that did not match these spectra although the same time resolution and temperatures were used in their stopped-flow studies.

The kinetics of intermediate formation has been studied also with P450cam in the absence and presence of substrates together

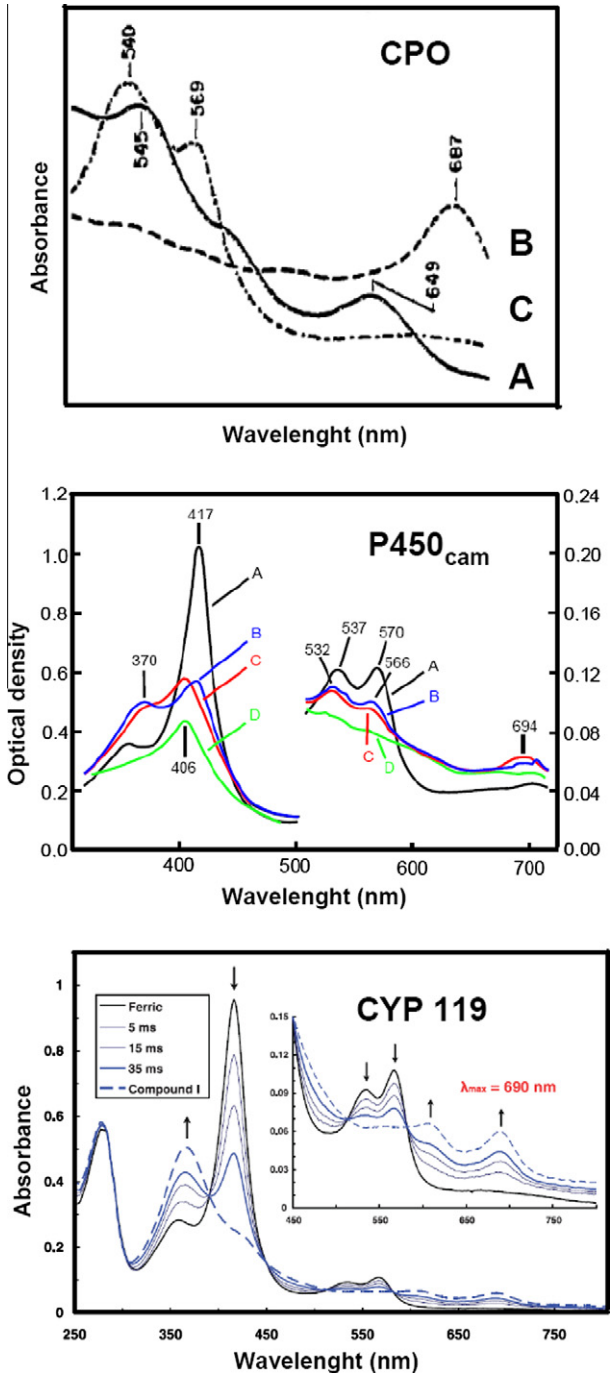

Fig. 5. Top: Visible absorption spectrum of the resting CPO (A) and its Cpd I (B), and Cpd II (C), reprinted from [43] with permission from Elsevier. Middle: UV–vis spectrum of a 10 μM low-spin ferric P450cam in 50 mM potassium phosphate buffer at pH 7 (A) and spectra recorded after addition of 300 μM *m*-CPBA after 6 ms (B), 25 ms (C) and 200 ms (D) reaction time, reprinted after [29] with permission from Elsevier. Bottom: UV/visible spectra obtained from the stopped-flow mixing (1:1) of 20 mM ferric CYP119 with 40 mM *m*-CPBA at 4 °C. The blue traces correspond to spectra taken 5, 15, and 35 ms after mixing. Maximum yield of P450-I was ~70% at 35 ms. The dashed line represents the spectrum of CYP119 Compound I obtained by difference techniques. From [9], reprinted with permission from AAAS.

with *m*-CPBA as oxidant under sub-stoichiometric concentrations [34]. For the substrate-free protein the rate for the reaction with H_2O_2 decreases with increasing pH (pK_a = 8.8) suggesting that a protonation/deprotonation equilibrium of presumably Tyr96 assists the intermediate formation because replacing this tyrosine by alanine removes this pH effect. For the reaction with *m*-CPBA a pK_a of 6.8 was obtained. The spectral shape for this intermediate has, however, not been resolved. Dawson and coworkers [35] have reported that in the reaction of P450cam with PA at pH >7 Cpd I is formed whereas at low pH only a species with a Soret band at 406 nm is observed, which they assigned to a Fe(IV)=O + tyrosyl radical species (named Cpd ES). Such an intermediate has also been detected by a combined Mössbauer- and EPR study reported by us [36,37] (see also Mössbauer spectroscopy section). However the studies of Dawson and coworkers have been performed with a 240-fold excess of PA (see Fig. 5 of [35]) which certainly should lead to fast degradation of the enzyme.

Green and coworkers [38] have recently tested how the spectra of the stopped-flow experiments performed by Sligar and coworkers [30] can be simply explained. By assuming so-called target spectra for complexes involved in the reaction they concluded that only two components (ferric form and Cpd I) are needed to completely simulate the reaction spectrum. In that study the authors also demonstrated that the spectrum obtained for the intermediate produced by the laser flash photolysis technique by Sheng et al. [39] represents very likely not that of P450 Cpd I. Very recently Rittle and Green performed a stopped-flow UV/visible study by mixing 20 μM highly purified ferric CYP119 with two equivalents of *m*-CPBA at 4 °C and pH 7 in potassium phosphate buffer. Under these conditions they were able to reproduce the results of Egawa et al. [29] and Kellner et al. [30] without using the single value decomposition method. Inspection of their data yields a well-defined band at 690 nm with its maximum intensity after 35 ms (Fig. 5). This is the first report in which an optical spectrum of P450 Cpd I could be directly and univocally identified.

Vibrational spectroscopy (resonance Raman, infrared)

In contrast to UV–vis. spectroscopy vibrational spectroscopy can give an insight into more local entities such as the iron–ligand bond which is important in particular for Cpd I. To observe, i.e., the Fe–O stretch vibration by infrared spectroscopy (IR) the Fe–O unit must have a strong dipole moment. This is the case for porphyrin Fe–O complexes and the Fe–O stretch vibration has been observed for a number of iron-oxo-porphyrin complexes [78]. However, for heme proteins the infrared spectra are too strongly overlapped by many bands from different parts of the protein and the protein concentration had to be very high to detect the Fe–O stretch band. An alternative technique is resonance Raman spectroscopy (RR). With this method one uses the advantage that during the transition to the excited electronic state structural properties are changed and therefore transitions between vibration states are enhanced. So, the vibration frequency is a property of the electronic ground state but the band intensity depends on the electronic transition which the laser light excites.

RR spectroscopy combined with oxygen isotope labeling has been applied on a large number of porphyrin model complexes showing that the proximal ligand largely determines the Fe=O stretch frequency [40,41]. However in heme proteins, the capability of distal side amino acids to provide a proton or hydrogen bond is very important. The Fe=O stretch vibration frequency for six-coordinated porphyrin model complexes with non-radical character of the porphyrin appears between 818 and 841 cm^{-1} [42]. If the porphyrin is a π-cation radical (Cpd I) this frequency shifts significantly to lower values at about 763 cm^{-1}.

For iron-oxo complexes in different heme proteins the Fe=O stretch vibration for Cpd II appears between 767 and 800 cm^{-1}. Interestingly, in CPO Cpd I, the Fe=O stretch vibration lies at 790 cm^{-1} [43] as already mentioned above (Fig. 6). The Fe=O stretch vibration for CPO Cpd II has not been found in RR spectra even not when different excitation wavelengths are used [26] up

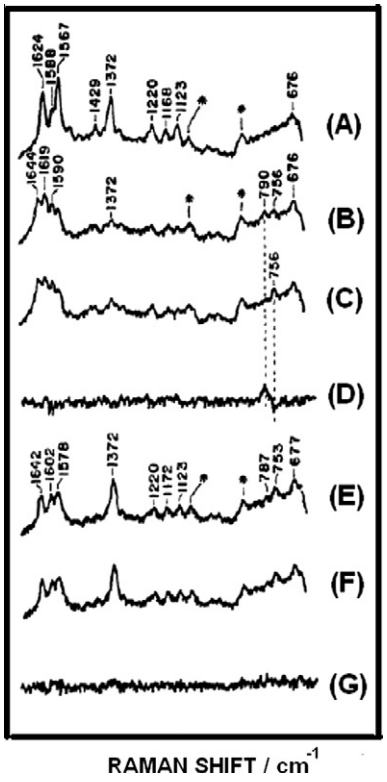

Fig. 6. Resonance Raman spectra of CPO: (A) Resting CPO. (B) Cpd I derived from reaction with $H_2{}^{16}O_2$, (C) and from reaction with $H_2{}^{18}O_2$. (D) Difference spectrum. (E) Cpd II derived from $H_2{}^{16}O_2$. (F) Cpd II derived from $H_2{}^{18}O_2$. (G) Difference spectrum. Reprinted from [43] with permission from Elsevier.

to the year 2006 when the Green group reported a ^{18}O and ^{2}H-sensitive Fe(IV)=O stretch at a low value as 565 cm^{-1} which points to the existence of an Fe(IV) hydroxide [44].

Up to now no IR spectroscopy data of P450 Cpd I and Cpd II have been reported, but a Fe=O stretch vibration at 834 cm^{-1} has been observed in a non-heme iron(IV)-oxo model complex (reaction product of Fe(II)-1,5,8,11-tetramethyl-1,4,8,11-tetraza-cyclotetradecane-CF_3SO_3 with iodosobenzene in CH_3CN). The IR spectrum of this complex shows a downshift by 34 cm^{-1} in the ^{18}O isotopomer [45].

Mixed-flow transient RR studies with a reconstituted P450cam system under catalytic conditions have been performed and reveal an O–O-stretch vibration signal very similar to the simple dioxygen complex, but no Fe–O-characteristic Raman signal at ~790 cm^{-1} was observed [46]. In order to find the Cpd I intermediate Fe=O stretch vibration, Sjodin et al. [47] measured the RR spectra of the oxygen complex of the wild-type and D251N mutant of P450cam in the presence of reduced putidaredoxin, the natural redox partner. However, also in these studies neither the stretch vibration for Fe=O nor for a peroxo or hydroperoxo complex was found.

Electron paramagnetic spectroscopy (EPR)

Electron paramagnetic spectroscopy (EPR) can measure the quantity and the properties (e.g., the ratio J/D where J and D are the exchange energy and the zero-field splitting, respectively) of half-integer spin Cpd I systems. The sample is subjected to a magnetic field B and the absorption of microwave radiation is measured as a function of the applied magnetic field strength. The resonance condition for a free electron with $S_{el} = 1/2$ is $h\nu = g_e \mu_B B$, with g_e being the electronic g-value ($g_e = 2.0023$) and μ_B the Bohr magneton. The resonance fields of a spin system in a molecule depend not only on the spin S itself, but also on the orientation of the molecule with respect to the applied field B because of spin–orbit interaction. Spin–orbit interaction is also responsible for lifting the degeneracy of a spin S, which would be $2S + 1$, in the case of no spin–orbit interaction in zero-magnetic field. Therefore effective g-factors called g_x, g_y, and g_z (or g_1, g_2, g_3) have been introduced which are characteristic for a given spin multiplet. Cpd I has a ferryl Fe(IV) species with spin $S_{Fe(IV)} = 1$ which is exchange coupled to a porphyrin radical with spin $S' = 1/2$. In the case of strong exchange coupling the total spin S_{tot} of a Cpd I intermediate can either be $S_{tot} = 1/2$ for the case of antiparallel (antiferromagnetic) spin coupling or $S_{tot} = 3/2$ for the case of parallel (ferromagnetic) spin coupling. X-band EPR ($\nu \sim 9.4$ GHz) is the ideal method to study half-integer spin systems and it is therefore the method of choice to determine the spin state of Cpd I reaction intermediates. In order to determine their ground state properties the measurements have to be performed at temperatures around 10 K. In order to get good signal to noise ratio it is advisable to work with enzyme concentrations in the range of 0.5–1 mM range. In principle EPR can be used as a fingerprint method since $S = 3/2$ species give EPR spectra with $(g_x + g_y)/2 = 4$ and $g_z = 2$ and $S = 1/2$ species are observed with all three g-values around 2. However in the case of weak exchange coupling or if the zero-field splitting D of the ferryl Fe(IV) is in the order of the exchange energy the analysis of EPR spectra is not as straightforward as stated above. For this case the observed g-values can be conveniently analyzed by means of the spin Hamiltonian formalism.

In order to describe EPR spectra (but also magnetic Mössbauer spectra) the spin Hamiltonian has been complemented by terms for exchange coupling and Zeeman interaction of the radical:

$$\hat{H}_{fs} = D\left[\hat{S}_z^2 - \frac{1}{3}S(S+1) + \frac{E}{D}\left(\hat{S}_x^2 - \hat{S}_y^2\right)\right] + \mu_B \vec{S}\overleftrightarrow{g}\vec{B} + \vec{S}\overleftrightarrow{J}S' + \mu_B \vec{S}'\overleftrightarrow{g}'\vec{B}. \quad (1)$$

The tensor quantity $\overleftrightarrow{J}$ describes the magnetic coupling tensor which acts between the radical spin $S' = 1/2$ and the $S_{Fe(IV)} = 1$ entity. If dipole contributions to the magnetic coupling are negligible $\overleftrightarrow{J}$ is diagonal and isotropic and the well-known Heisenberg exchange coupling term $J_0\vec{S}'\vec{S}$ is obtained. $J_0 < 0$ leads to antiparallel coupling ($S_{tot} = 1/2$) and $J > 0$ to parallel ($S_{tot} = 3/2$) spin coupling, but note that also other conventions concerning the sign of J are used [48]. The electronic coupling tensor $\overleftrightarrow{J} = 1 \bullet J_0 + \overleftrightarrow{J}_a$ consists of an isotropic part J_0 and a traceless anisotropic tensor $\overleftrightarrow{J}_a$ which takes the dipole–dipole interaction between ferryl and porphyrin radical spin into account. The components of $\overleftrightarrow{J}_a$ as well as the local g-tensor of the ferryl iron and its zero-field splitting parameters D (axial) and E (rhombic) with the rhombicity parameter E/D have been determined for the first time for Cpd I of CPO by Rutter et al. [49].

The EPR spectra of ferric cytochrome P450cam and CPO exhibit an anisotropic EPR signal within the $g \sim 2$ region corroborating their $S = 1/2$ state (2.62, 2.27, 1.843 for CPO, and 2.45, 2.26, 1.91 for substrate-free P450cam). When CPO reacts with PA within 8 ms the EPR spectrum of the frozen reaction mixture does clearly show an axial $S = 1/2$ signal with $g_{||} \sim 2.00$ and $g_{\perp} \sim 1.75$ typical for a Cpd I with a $S_{tot} = 1/2$ ground state [50] (Fig. 7a).

For Cpd I of CPO the strength of the Heisenberg exchange interaction (J_0) is of similar magnitude as the zero-field splitting D of the ferryl iron $S = 1$ system. Fig. 7 shows the calculated g-factors of an axial Cpd I system with zero rhombicity ($E/D = 0$) based on the Hamiltonian given above. Comparing the plot given in Fig. 8 with the experimentally observed g-values a value of $J_0/D \sim 1$ can be obtained. This is corroborated by the corresponding spin-Hamiltonian simulation of the Cpd I signal shown in Fig. 7a performed

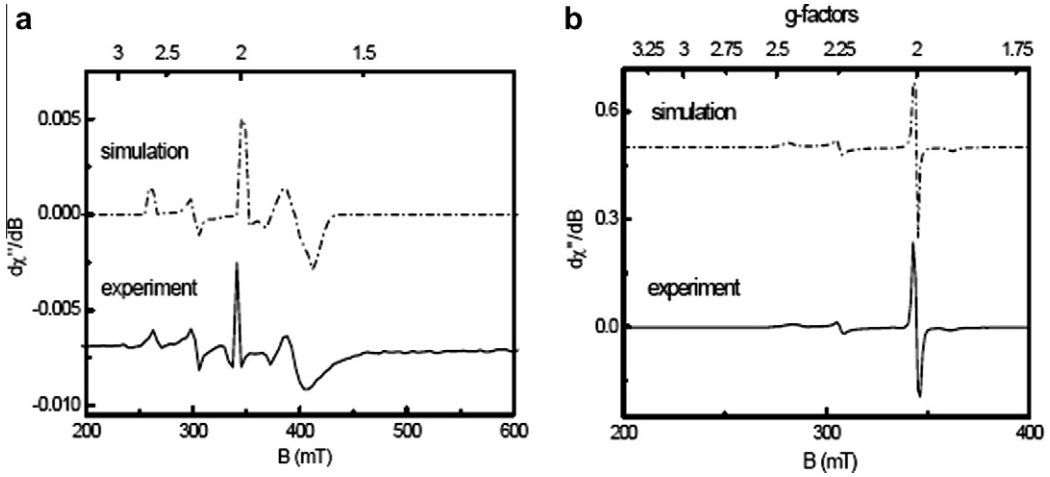

Fig. 7. X-band EPR spectra taken at 20 K of (a) ^{56}Fe-CPO freeze-quenched with PA (8 ms reaction time). 5 mM sodium acetate buffer, pH 4.8. PA (5 mM) to CPO (1 mM) ratio of 5: 1 were mixed to give half of each concentration in the mixture. The dashed-dotted line is a simulation assuming two components: the signal of the starting material (*g*-values 1.84, 2.27, and 2.62 and relative contribution 30%) and the signal of Cpd I (spin-Hamiltonian simulation with parameters given in the text; relative contribution 70%). (b) substrate-free cytochrome ^{57}Fe-P450cam freeze-quenched with peroxy acetic acid (PA) (8 ms reaction time). 100 mM potassium phosphate buffer, pH 7. PA (5 mM): P450 (1 mM) ratio of 5: 1 were mixed to give half of each concentration in the mixture. The dashed-dotted line is a simulation assuming two components: the signal of the starting material (*g*-values 1.91, 2.26, and 2.45 and relative contribution 85%) and the signal of a radical ($g = 2$; relative contribution 15%). For further experimental parameters see [36]. Reprinted from [36] with permission from Elsevier.

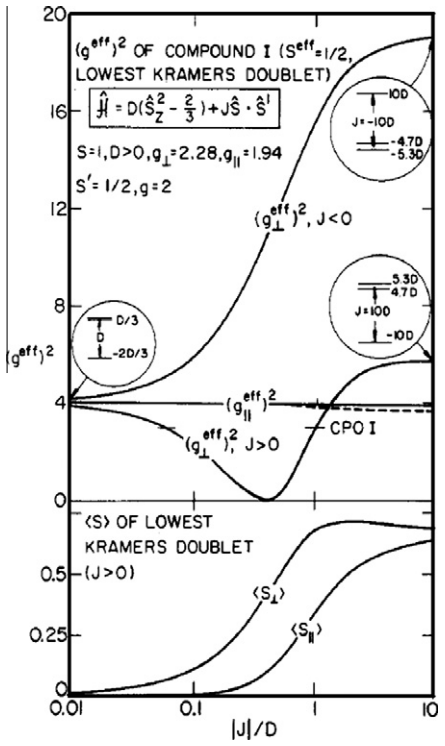

Fig. 8. Squares of calculated effective g values, $(g_{\|eff})^2$ and $(g_{\perp eff})^2$ of a spin-coupled pair with $S = 1$ and $S' = 1/2$ as a function of $|J|/D$ for the lowest Kramers doublet. The model assumes a positive axial zero-field splitting D of the ferryl spin $S = 1$ and an isotropic exchange interaction between S and the porphyrin radical spin $S' = ½$.The values adopted for the ferryl *g*-tensor are those predicted for $D/k = 52$ K by the model of Oosterhuis and Lang. Adapted with permission from [49]. Copyright 1984 American Chemical Society.

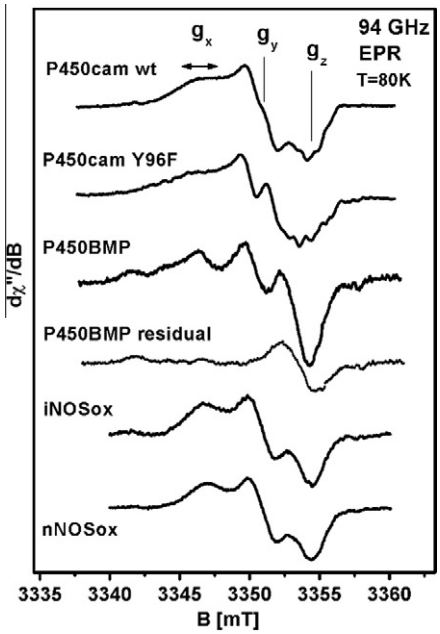

Fig. 9. 94 GHz EPR spectra of P450cam wild-type, P450cam-Y96F, P450BMP, iNOSox, and nNOSox. All samples were freeze-quenched after 8 ms reaction with peroxy acetic acid. Experimental parameters in [36,37,56,57]. Reprinted with permission from [57].

by us which yields $J_0/D = 0.97$ [36] and is essentially the same as the value given by Rutter et al. [49].

Fig. 7b shows the EPR spectrum obtained from substrate-free P450cam, which reacted with PA within 8 ms. The spectrum does not show a signal attributable to a magnetically coupled Cpd I species. Instead, the pattern of the starting material is superimposed on a strong radical signal. The latter has been assigned to Tyr96, which is 9.4 Å from the heme iron [37].

In order to unequivocally identify and assign the observed radicals in P450 freeze-quenched samples were investigated using 94, 190, and 285 GHz EPR [51]. At theses frequencies all three *g*-components were resolved in the spectra. For the radicals in all samples similar *g*-values were obtained, $g_x = 2.0078–2.0064$, $g_y = 2.0044$ and $g_z = 2.0022$, which are fingerprints for tyrosyl radicals [52–55]. Based on the 94 GHz EPR-spectra (Fig. 9) a detailed assignment was performed. Two classes of protons give rise to the observed hyperfine couplings in tyrosine radicals, i.e., the

ring-protons (α-protons) and the β-protons of the side chain. A large hyperfine coupling arises from one of the two β-protons of the side chain. This coupling exhibits only a small anisotropy and its isotropic value, $A_{iso}(H_\beta)$, does not only depend on the π-spin density ρ^{π}_{C} of the adjacent π-carbon, but is also strongly dependent on the geometry of the side chain, according to

$$A_{iso}(H_\beta) = \rho^{\pi}_{C}(B' + B'' \cos^2\theta) \quad (2)$$

where B' and B'' are empirical constants and θ is the dihedral angle between the axis of the π-orbital (p_z) of the adjacent carbon atom and the projected $C_\beta H_\beta$ bond. From the simulation of the 94 GHz EPR spectrum of the P450cam wild type and mutant proteins (Fig. 9) isotropic hyperfine value, $A_{iso}(H_{\beta 1})$ for one of the β-CH_2 protons have been obtained. Using these values combined with $\rho^{\pi}_{C1} = 0.38$, $B' = 0$ and $B'' = 5.0$ mT dihedral angles θ_1 were calculated, which matched very well the angles obtained for Y96 (41°) in the wild type crystal structure of substrate-free P450cam and for Y75 (26°) in the mutant Y96F of P450cam. However, for the Y96F-Y75F double mutant no radical of an amino acid side chain was seen [51]. Interestingly, also for P450BMP and NOS tyrosine radicals have been observed further including contributions of tryptophan radicals [56,57].

If the radical spin of Cpd I is only weakly coupled to the ferryl spin very broad EPR traces are observed around $g \sim 2$ at temperatures below 10 K. This is the case for horseradish peroxidase Cpd I. In a combined EPR and Mössbauer study the Debrunner group reported a coupling tensor $\underleftrightarrow{J}/k_B = (-4, -2, 6)$ K which represents a relatively weak exchange interaction [58,59].

The analysis of the effective g-factors of a Cpd I EPR spectrum does yield the ratio $|J|/D$. The exchange coupling strength J on the other hand can be estimated from measuring the half-saturation power behavior $P_{1/2}$ of the EPR signal resulting from the lowest Kramers doublet as a function of temperature [49]. Since this method requires an exact temperature calibration of an EPR-cryostat which is not easily achieved, it is advisory to use complimentary methods like Mössbauer spectroscopy. In conclusion it can be stated that a full range of spin-coupling behaviors has been seen with the sets of Cpds I observed to date, from antiferromagnetic coupling (CPO [49,50] and P450 CYP119 [9]) over weak coupling (HRP [58,59]) to ferromagnetic coupling (catalases [60]). It is the general consensus now that all these Cpd I species have Fe(IV)–porphyrin-π-cation radical character, since Davydov and coworkers showed by electron-nuclear double resonance spectroscopy (ENDOR) that no major radical delocalization on the axial sulfur exists at least in Cpd I of CPO [61].

Mössbauer spectroscopy

Mössbauer spectroscopy as a nuclear spectroscopy makes use of the 14.4 keV transition between the ground and the first excited state of the ^{57}Fe-nucleus. In a conventional Mössbauer spectrometer, the 14.4 keV radiation is produced by a radioactive ^{57}Co-source and the energy is scanned by moving the source with the Doppler velocity v within an interval of up to ±500 neV which corresponds to a Doppler velocity of ±10 mms^{-1}. Since the natural abundance of ^{57}Fe is only 2% Mössbauer studies on iron proteins require isotopic enrichment which nowadays can be achieved by growing the expression system in media which have only ^{57}Fe salts added. This drawback is compensated by the fact that Mössbauer spectroscopy detects all iron species in a reaction mixture and if Mössbauer samples are prepared by the RFQ-technique not only the putitative Cpd I species but also the amount of Cpd II or not reacted enzyme can be identified and quantified.

The ferryl Fe(IV) state of both Cpd I and Cpd II species have both very characteristic isomer shifts of $\delta \sim 0$ mm/s and quadrupole splittings of $\Delta E_Q \sim 1$–2 mm/s (see Table 1). If Mössbauer spectra of Cpd II are measured at liquid helium temperatures in weak applied magnetic fields of ~10–20 mT the ferryl iron exhibits only a quadrupole doublet without an observable magnetic splitting. This is an intrinsic property of an $S = 1$ system with a high positive zero-field splitting D and is observed in all Mössbauer studies of Cpd II intermediates and models observed to date. Once an even weak exchange coupling like in Cpd I of HRP is present the Mössbauer spectrum obtained under the same conditions displays a slight asymmetric doublet. If the exchange coupling is in the order of the zero-field splitting of the ferryl Fe(IV) $S_{Fe(IV)} = 1$ system a complicated 4-line pattern is observed for Cpd I intermediates with $S_{tot} = 1/2$ ground state (like CPO) but also for Cpd I models with parallel spin coupling and $S_{tot} = 3/2$ ground state. In order to determine the exchange coupling J and the zero-field splitting D from Mössbauer spectroscopy spin expectation values $\langle S \rangle$, on the basis of the electronic spin Hamiltonian (Eq. (1)) have to be calculated and subsequently used in order to simulate the experimentally observed magnetic Mössbauer spectra at best taken under different field conditions.

The simulation of paramagnetic Mössbauer spectra is based on the following usual nuclear Hamiltonian:

$$\hat{H}_i = \frac{eQV_{zz}}{4I(2I-1)}\left[3\hat{I}_z^2 - I(I+1) + \eta\left(\hat{I}_x^2 - \hat{I}_y^2\right)\right] - g_N\mu_N\vec{B}_0\vec{I} + \langle S\rangle_i \underleftrightarrow{A}\vec{I} \quad (3)$$

In Eq. (3) I denotes the nuclear spin, Q is the nuclear quadrupole moment of the excited nuclear state of ^{57}Fe, V_{zz} is the main component of the electric-field gradient tensor, which gives rise to the quadrupole splitting and $\eta = (V_{xx} - V_{yy})/V_{zz}$ is the asymmetry parameter of the electric-field gradient. A denotes the hyperfine coupling tensor, g_N is the nuclear g-factor, μ_N is the nuclear magneton and $\vec{B}$ is the applied field.

The Mössbauer spectrum obtained after reaction of substrate-free P450cam with a fivefold excess of PA contains approximately 87% ferric low-spin iron with the same g-factors and hyperfine parameters as the substrate-free P450cam starting material, upon which is superimposed by a quadrupole doublet with $\delta = 0.13$ mms^{-1} and $\Delta E_Q = 1.94$ mms^{-1}. The isomer shift of this doublet is indicative of ferryl iron with $S_{Fe(IV)} = 1$ [37]. The fact that this doublet does not exhibit magnetic hyperfine splitting within a moderate field of 1 T is consistent with an $S_{Fe(IV)} = 1$ system with positive zero-field splitting parameter D and indicates that the ferryl iron is not taking part in a spin-coupled (ferromagnetic or antiferromagnetic) system.

Cpd I of CPO on contrast shows a characteristic four line pattern at $T = 4.2$ K and a weak external field of 34 mT perpendicular to the γ-ray. (Fig. 10b, left). The line intensity ratio depends strongly on the direction of the magnetic field (Fig. 10a, left) and can be reproduced satisfactorily by means of the Hamiltonians given in Eqs. (1) and (3). Consistent with the EPR analysis which leads to $|J/D| \sim 1$ the Mössbauer trace could be reproduced with the following parameters: an exchange coupling constant of $J = 1.02D$; a zero-field splitting of the ferryl iron $D = 52$ K and a rhombicity parameter of $E/D = 0.035$, an isomer shift of $\delta = 0.15$ mm/s, a quadrupole splitting $\Delta E_Q = 1.02$ mms^{-1} and an axial $\underleftrightarrow{A}$-tensor of the ferryl iron with $A_{x,y}/g_N\,\mu_N = -20.2$ T and $A_{x,y}/g_N\,\mu_N = -6$ T. It is intriguing that the Mössbauer signature of CYP119 Cpd I obtained under comparable experimental conditions is very similar to that of Cpd I of CPO (Fig. 10, right) [9]. This observation together with the g-values observed by EPR (1.96,1.86, 2.00, Table 1) shows unambiguously that Cpd I of CYP119 can be trapped by freeze–quench techniques in high yields and that it has a $S = 1/2$ ground state. Indeed, Cpd I of CYP119 exhibits $\delta = 0.11$ mm/s and $\Delta E_Q = 0.90$ mm/s and also the $\underleftrightarrow{A}$-tensor of the ferryl iron is comparable to that of CPO (Table 1).

Table 1
Spectral parameters of Cpd I of selected heme proteins and porphyrin model complexes.

Species	EPR			UV–vis spectroscopy	Resonance Raman spectroscopy	Mössbauer spectroscopy						EXAFS
	S	$\overleftrightarrow{g}_{eff}$	$\lvert J/D_{Fe(IV)}\rvert$	Band positions (nm)	$\nu(Fe^{IV}–O)$ (cm^{-1})	δ (mms^{-1})	ΔE_Q (mms^{-1})	$\overleftrightarrow{g}_{Fe(IV)}$	$D_{Fe(IV)}$ (cm^{-1})	$E/D_{Fe(IV)}$	$\overleftrightarrow{A}/g_N\mu_N$ (T)	Fe–O distance (Å)
$[Fe^{IV}{=}O(TMP^{\cdot})]^{+}$[a] [28,78]	3/2	$\begin{pmatrix}4.47\\3.50\\1.98\end{pmatrix}$	1.72	406, 674		0.08	1.62	$\begin{pmatrix}2.21\\2.23\\1.99\end{pmatrix}$	25	0.04	$\begin{pmatrix}-25\\-25\\-5\end{pmatrix}$	1.64–1.66
$[Fe^{IV}{=}O(PLAC^{\cdot})]^{+}$[b] [79]	3/2	$\begin{pmatrix}3.16\\3.64\\1.99\end{pmatrix}$	0.55	406, 730	836	0.08	1.66	$\begin{pmatrix}2.17\\2.17\\1.99\end{pmatrix}$	20	0.1	$\begin{pmatrix}-17.5\\-17.5\\-10\end{pmatrix}$	
CPO Cpd I [36,49,43,44]	1/2	$\begin{pmatrix}1.73\\1.73\\2\end{pmatrix}$	~1.0	367, 610, 666	790	0.15	1.02	$\begin{pmatrix}2.28\\2.28\\1.94\end{pmatrix}$	35	0.035	$\begin{pmatrix}-20.2\\-20.2\\-6\end{pmatrix}$	1.65
HRP Cpd I [58,80]	1/2	~2	~0.1	400, 577,622, 651	790	0.08	1.25	$\begin{pmatrix}2.25\\2.25\\1.98\end{pmatrix}$	25.7	0	$\begin{pmatrix}-19.3\\-19.3\\-6\end{pmatrix}$	1.64–1.67
Catalase Cpd I *P. mirabilis* [75,81]	1/2		0.31	405, 660		0.12	1.09	$\begin{pmatrix}2.0\\2.0\\2.0\end{pmatrix}$	17.2	0	$\begin{pmatrix}-18.9\\-18.9\\-5.4\end{pmatrix}$	
Catalase Cpd I *M. lysodeikticus* [60]	3/2	$\begin{pmatrix}3.32\\3.32\\2\end{pmatrix}$										
P450cam Cpd I [29]	?			367, 694								
P450 CYP 119 Cpd I [30,9]	1/2	$\begin{pmatrix}1.96\\1.86\\2\end{pmatrix}$	1.3	370, 690		0.11	0.90	$\begin{pmatrix}2.27\\2.20\\2.0\end{pmatrix}$			$\begin{pmatrix}-20\\-23\\-3\end{pmatrix}$	

[a] TMP, tetramesityl porphyrin.
[b] PLAC, 2-oxa-3-oxotetrakis(2,6-dichlorophenyl) porphine; HRP, horseradish peroxidase; CPO, chloroperoxidase.

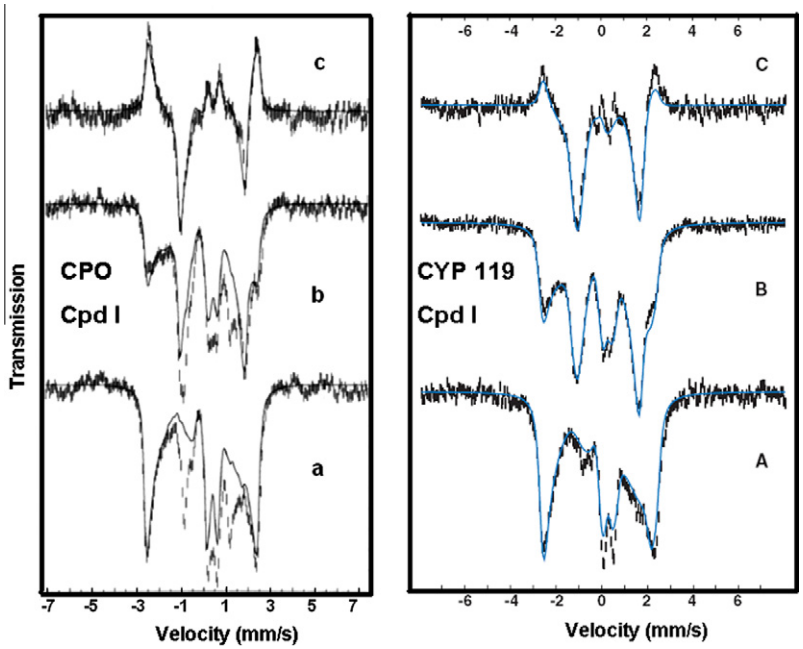

Fig. 10. Left: Mössbauer spectra of CPO Cpd I as reported by Rutter et al. [49]. The spectra were taken at 4.2 K in an applied field of 34 mT (a) parallel and (b) perpendicular to the direction of the beam of gamma rays. In both traces the spectral contribution of the native enzyme has been subtracted. There is still a misfit between simulation and experiment which has been tentatively assigned to a doublet with $\delta = 0.1$ mm/s and $\Delta E_Q = 2.2$ mm/s. The line intensities of this doublet do not depend on the direction of the external magnetic field. Therefore the authors showed also the difference spectrum in trace c, $(c) = (b) - (a)$. Parameters are given in Table 1. Right: Mössbauer spectra of CYP 119 Cpd I as reported by Rittle and Green taken under comparable experimental conditions as the spectra of CPO Cpd I [9]. The simulations are based assuming an effective $S = 1/2$ representation with parameters given in Table 1. CYP 119 Cpd I was prepared by mixing (2:1) ferric CYP119 (3 mM, in 100 mM potassium phosphate buffer, pH 7.0) with a solution of *m*-CPBA (12 mM, in 20:80 acetonitrile/water). Reprinted with permission from [49]. Copyright 1984 American Chemical Society. From [9], reprinted with permission from AAAS.

Nuclear inelastic scattering (NIS)

Nuclear inelastic scattering of synchrotron radiation (also called nuclear resonance vibrational spectroscopy; NRVS) can be regarded as an extension of the conventional, energy-resolved Mössbauer spectroscopy to energies of the order of molecular vibrations [62,63]. In contrast to a nuclear forward scattering (NFS) – experiment – which can be regarded as Mössbauer spectroscopy in the time domain – the energy of the incoming radiation E_γ is varied within an interval of up to ±100 meV around the resonance energy $E = 14.4$ keV of the Mössbauer nucleus. In a NIS-experiment the absorption probability is measured as a function of the energy difference $E - E_\gamma$. An advantage of the NIS technique when compared to other vibrational spectroscopies is that it is a site-selective method, which solely detects the dynamics of the active site iron. From the experimental data it is possible to calculate the partial density of phonon states (PDOS) which represents those modes involving iron motion. The intensity of the individual peaks in the PDOS is roughly proportional to the mean-square displacement of the Mössbauer nucleus arising from the corresponding molecular vibration. Different from IR- or Raman spectroscopy, NIS spectra depend solely on mechanical properties, i.e., the eigenfrequencies and eigenvectors of the vibrations, but not on electrical properties like the polarizability of the molecule [64]. For this reason NIS can be calculated by theoretical methods with good reliability.

NIS has not been applied to Cpd I species so far, but Sage and coworkers report a NIS study on high-valent Fe(IV) oxymyoglobin [65]. By means of this method it was possible to detect a Fe(IV)═O stretching mode at 805 cm^{-1} (see Fig. 11). Reduction to the ferric state and protonation of the iron-oxo unit result in a downshift of the Fe–O stretching frequency from 805 to 556 cm^{-1}. Because the NIS spectroscopy gives direct access to an important parameter, the Fe–O stretching frequency, it would be a challenge to apply this technique to P450, too.

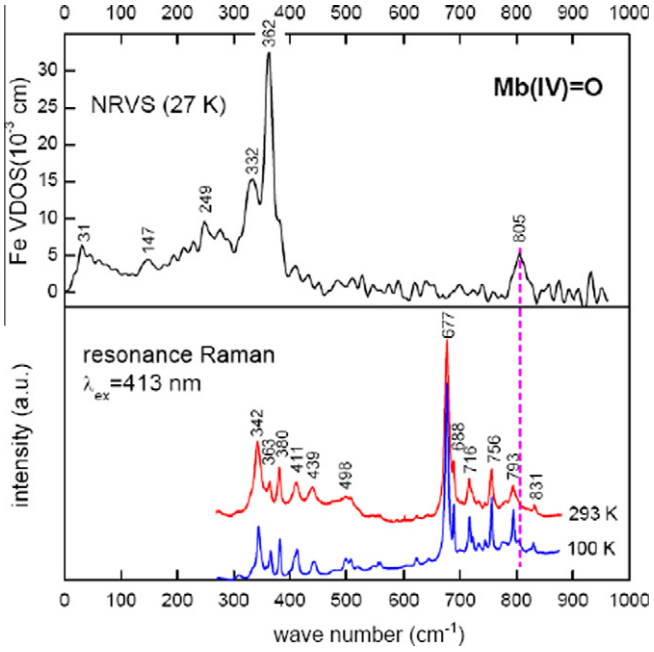

Fig. 11. Comparison between NIS (NRVS) data (top) and resonance Raman spectra for Mb(IV)═O. The dashed vertical line identifies the line position of the $(Fe(IV)═O)^{2+}$ stretching mode at 805 cm^{-1}. This mode is clearly visible in the NIS spectrum, but is strongly overlayed by other bands in the resonance Raman spectrum. Reprinted with permission from [65] (Supplementary information). Copyright 2008 American Chemical Society.

Extended X-ray absorption fine structure (EXAFS)

The position of the X-ray absorption edge of an element is characteristic for its valence state. The extended region the X-ray absorption edge has a damped periodic fine structure which depends on the number and especially the distance to its ligand atoms. This extended X-ray absorption fine structure (EXAFS) is caused by a quantum mechanical effect namely the superposition of the incoming X-ray beam and the photoelectrons emitted during the absorption process. This synchrotron based technique measures especially metal ligand distances with very high accuracy of at best one-hundredth of an Ångstrom and it requires sample volumes of approximately 50–100 μl and metal concentrations of at least 100 μM.

One important proof for the existence of an iron-oxo intermediate is the measurement of the Fe=O bond distance which can be done by EXAFS studies. For heme proteins other than thiolate heme proteins, i.e., HRP [66], EXAFS studies revealed a Fe=O distance of ~1.61–1.64 Å for Cpd I as well as Cpd II which matches values known from model porphyrin complexes. Recently, HRP was studied again by EXAFS yielding a Fe=O distances for Cpd I and Cpd II of 1.67 Å and 1.70 Å, respectively [67]. The uncertainty in the distance determination lies at ±0.02 Å. The same authors measured CPO Cpd II produced by rapid-mixing CPO with PA and ascorbate and freeze-quenching the intermediate in isopentane. A Fe=O distance of 1.82 Å was determined by fitting the EXAFS data. This unusually large distance was taken as indication that the oxygen atom should be protonated. Because CPO was found to be able to catalyze hydroxylations [68] it was argued that CPO Cpd II might be a good model for P450 Cpd I which has abstracted a hydrogen from the substrate according to the "radical rebound" model [69].

EXAFS studies on P450 and NOS have only been performed for the ferric and ferrous forms in the presence and absence of substrates [70–72]. However to our knowledge no EXAFS data for intermediate species have been reported so far.

X-ray crystallography

The only crystal structure of reaction intermediate species in thiolate heme proteins has been resolved for P450cam by Schlichting et al. [73] by using the radiolytic ability of the X-rays to produce solvated electrons. The dioxygen complex of P450cam was produced by dithionite reduction of the protein in the crystal. The second electron was then provided by radiolysis at cryogenic temperatures. An electron density in a distance of 1.65 Å to the heme iron was found and assigned to the oxygen atom of a putative iron-oxo species because the hydroxylation product 5-exo-hydroxycamphor was detected by gas chromatography after thawing the crystal and product extraction. This Fe=O distance is in a range expected for Cpd I species similar to that observed by time-resolved X-ray diffraction studies on Cpd I intermediates in cytochrome c peroxidase [74] and catalase [75]. However, an iron coordinated water molecule can not be excluded as origin for this electron density.

Outlook

Summarizing, it has been unambiguously shown at least for one P450 (thermostable CYP119) that Cpd I can be trapped in the shunt pathway within several tens of milliseconds. Cpd I can be obtained in high yields and its marker band around 690 nm is detectable in the UV–vis spectrum without any multicomponent fitting analysis. Its electronic ground state is very similar to the Fe(IV)-oxo porphyrin radical in CPO. Compounds I of CYP119 and CPO have the same ground state spin $S = 1/2$ and a comparable Heisenberg exchange coupling strength between the ferryl and the porphyrin radical spin. Importantly, Rittle and Green also defined the absolute kinetic properties of Cpd I in oxygenating reactions of substrates and determined the kinetic isotope effects for this process, thereby proving the chemical competence of Cpd I in P450 metabolism [9].

However, it remains mysterious why Cpd I can apparently not be trapped in significant quantities in other P450s. In fact also with the Y96F-Y75F double mutant of P450cam it has been not possible to accumulate Cpd I in significant amounts using the shunt reaction which is evident from the absence of the porphyrin π-cation radical marker band around 690 nm. Obviously, Cpd I of P450cam is so highly reactive that it does not accumulate because reaction rates are faster than formation rates. Even injection of the second electron into the ternary complex of camphor, O_2, and ferro-cytochrome P450cam at 77 K by γ-radiation followed by annealing around 210 K did not reveal a species with an EPR spectrum corresponding to Cpd I but rather to the hydroxycamphor P450cam-complex indicating product formation. Indeed, 5-exo-hydroxycamphor has been afterwards detected in the sample in a γ-radiation dose-dependent manner by gas chromatography [21].

The answer lies certainly in the dynamics of the P450 structure. It has been recently argued that Cpd I is one of several branch points in the reaction cycle of P450 where a number of competing reactions take place such as the oxygen insertion into the substrate and individual leakage processes such as an oxidase reaction, protein radical formation, heme destruction, reaction with a second molecule of the used oxygen species, i.e., in the shunt pathway, and perhaps other as yet unknown reactions [76,77]. The amount of accumulation of Cpd I depends on the relative rate constants of the various competing reactions which finally determine the probability to detect Cpd I by the different spectroscopic technique. Obviously, future work might be no longer focused on the question as to whether Cpd I really exists in P450s but rather attempts to answer which structural and dynamical properties of the P450 conformation are required to trap Cpd I.

Acknowledgments

The diverse studies on cytochrome P450 were funded by the Deutsche Forschungsgemeinschaft grants Ju229/4-(1-3), Ju229/5-1, Sk35/3-(3-5) to C.J.; Schu1251/3-1 and Schu1251/11-1 to V.S. The authors thank all former co-workers and students, in particular J. Contzen, M. Richter, R. Christmann, C. Balluff, and Annegret Ahrens-Botzong, for contributing to projects related to the subject of this review. Special gratitude goes to A.X. Trautwein and F. Lendzian for the fruitful collaboration over many years in studying P450 intermediates. This review article has been dedicated to Professor Minor J. Coon on the occasion of his upcoming 90th birthday. Since more than 40 years C.J. has followed the significant contributions to the P450 field made by Jud and his coworkers and students. C.J. thanks him for all the interesting scientific contributions and discussions at the various P450 conferences.

References

[1] P.R. Ortiz de Montellano, Cytochromes P450 – Structure, Mechanism, and Biochemistry, third ed., Kluwer Academic/Plenum Publishers, New York, 2005.
[2] D.R. Nelson, Biochim. Biophys. Acta 1814 (2011) 14–18.
[3] T.L. Poulos, B.C. Finzel, A.J. Howard, J. Mol. Biol. 195 (1987) 687–700.
[4] J.T. Groves, G.A. McClusky, J. Am. Chem. Soc. 98 (1976) 859–861.
[5] J.T. Groves, R.C. Haushalter, M. Nakamura, T.E. Nemo, B.J. Evans, J. Am. Chem. Soc. 102 (1981) 2884–2886.
[6] J.T. Groves, J. Inorg. Biochem. 100 (2006) 434–447.
[7] D. Dolphin, R.H. Felton, Acc. Chem. Res. 7 (1974) 26–32.
[8] D. Dolphin, Philos. Trans. R. Soc. Lond. B 311 (1985) 579–591.
[9] J. Rittle, M.T. Green, Science 330 (2010) 933–937.
[10] H.B. Dunford, J.S. Stillman, Coord. Chem. Rev. 19 (1976) 187–251.
[11] H.B. Dunford, Heme Peroxidases, John Wiley & Sons, New York, 1999.

[12] H.B. Dunford, Peroxidases and Catalases: Biochemistry, Biophysics, Biotechnology and Physiology, second ed., John Wiley & Sons, New York, 2010.
[13] D.P. Ballou, G.A. Palmer, Anal. Chem. 46 (9) (1974) 1248–1253.
[14] S. De Vries, Freeze–quench kinetics, in: R.A. Scott, C.M. Lukehart (Eds.), Application of Physical Methods to Inorganic and Bioinorganic Chemistry, John Wiley & Sons, 2007, pp. 125–142.
[15] A.V. Cherepanov, S. De Vries, Biochim. Biophys. Acta 1656 (1) (2004) 1–31.
[16] M. Tanaka, K. Matsuura, S. Yoshioka, S. Takahashi, K. Ishimori*, H. Hori, I. Morishima, Biophys. J. 84 (3) (2003) 1998–2004.
[17] J. Pierre, M. Bazin, P. Debey, R. Santus, Eur. J. Biochem. 124 (1982) 533–537.
[18] M. Bazin, J. Pierre, P. Debey, R. Santus, Eur. J. Biochem. 124 (1982) 539–544.
[19] P.D. Nyman, P.G. Debrunner, J. Inorg. Biochem. 43 (1991) 346.
[20] R. Davydov, R. Kappl, J. Hüttermann, J.A. Peterson, FEBS Lett. 295 (1991) 113–115.
[21] R. Davydov, T.M. Makris, V. Kofman, D.E. Werst, S.G. Sligar, B.M. Hoffman, J. Am. Chem. Soc. 123 (7) (2001) 1403–1415.
[22] I.G. Denisov, M. Thomas, T.M. Makris, S.G. Sligar, J. Biol. Chem. 276 (2001) 11648–11652.
[23] R. Zhang, R.E.P. Chandrasena, E. Martinez II, J.H. Horner, M. Newcomb, Org. Lett. 7 (2005) 1193–1195.
[24] M. Newcomb, R. Zhang, R. Esala, P. Chandrasena, J.A. Halgrimson, J.H. Horner, T.M. Makris, S.G. Sligar, J. Am. Chem. Soc. 128 (14) (2006) 4580–4581.
[25] M.M. Palcic, R. Rutter, T. Araiso, L.P. Hager, H.B. Dunford, Biochem. Biophys. Res. Commun. 94 (1980) 1123–1127.
[26] T. Egawa, D.A. Proshlyakov, H. Miki, R. Makino, T. Ogura, T. Kitagawa, Y. Ishimura, J. Biol. Inorg. Chem. 6 (2001) 46–54.
[27] H. Fujii, J. Am. Chem. Soc. 115 (1993) 4641–4648.
[28] D. Mandon, R. Weiss, K. Jayaraj, A. Gold, E. Bill, A.X. Trautwein, Inorg. Chem. 31 (1992) 4404–4409.
[29] T. Egawa, H. Shimada, Y. Ishimura, Biochem. Biophys. Res. Commun. 201 (1994) 1464–1469.
[30] D.G. Kellner, S.-C. Hung, K.E. Weiss, S.G. Sligar, J. Biol. Chem. 277 (2002) 9641–9644.
[31] T.C. Pederson, R.H. Austin, I.C. Gunsalus, Redox and ligand dynamics in P450cam–putidaredoxin complexes, in: V. Ullrich, I. Roots, A. Hildebrandt, R.W. Estabrook (Eds.), Microsomes and Drug Oxidations, Pergamon Press, Oxford, 1977, pp. 275–283.
[32] G.C. Wagner, M.M. Palcic, H.B. Dunford, FEBS Lett. 156 (1983) 244–248.
[33] S.G. Sligar, B.S. Shastry, I.C. Gunsalus, Oxygen reactions of the P450 heme protein, in: V. Ullrich, I. Roots, A. Hildebrandt, R.W. Estabrook (Eds.), Microsomes and Drug Oxidations, Pergamon Press, Oxford, 1977, pp. 202–209.
[34] S. Prasad, S. Mitra, Biochem. Biophys. Res. Commun. 314 (2004) 610–614.
[35] T. Spolitak, J.H. Dawson, D.P. Ballou, J. Biol. Chem. 280 (2005) 20300–20309.
[36] V. Schünemann, C. Jung, J. Terner, A.X. Trautwein, R. Weiss, J. Inorg. Biochem. 91 (2002) 586–596.
[37] V. Schünemann, C. Jung, A.X. Trautwein, D. Mandon, R. Weiss, FEBS Lett. 479 (2000) 149–154.
[38] J. Rittle, J.M. Younker, M.T. Green, Inorg. Chem. 49 (2010) 3610–3617.
[39] X. Sheng, J.H. Horner, M. Newcomb, J. Am. Chem. Soc. 130 (2008) 13310–13320.
[40] H. Fujii, Coord. Chem. Rev. 226 (2002) 51–60.
[41] J.R. Kincaid, Resonance Raman spectra of heme proteins and model compounds, in: K.M. Kadish, K.M. Smith, R. Guilard (Eds.), The Porphyrin Handbook 7, Academic Press, New York, 2000, pp. 225–291.
[42] K. Nakamoto, Coord. Chem. Rev. 226 (2002) 153–165.
[43] T. Egawa, H. Miki, T. Ogura, R. Makino, Y. Ishimura, T. Kitagawa, FEBS Lett. 305 (1992) 206–208.
[44] K.L. Stone, R.K. Behan, M.T. Green, Proc. Natl. Acad. Soc. 103 (33) (2006) 12307–12310.
[45] J.-U. Rohde, J.-H. In, M.H. Lim, W.W. Brennessel, M.R. Bukowski, A. Stubna, E. Münck, W. Nam, L. Que Jr., Science 299 (2003) 1037–1039.
[46] T. Egawa, T. Ogura, R. Makino, Y. Ishimura, T. Kitagawa, J. Biol. Chem. 266 (1991) 10246–10248.
[47] T. Sjodin, J.F. Christian, I.D.G. Macdonald, R. Davydov, M. Unno, S.G. Sligar, B.M. Hoffman, P.M. Champion, Biochemistry 40 (2001) 6852–6859.
[48] J. Antony, M. Grodzicki, A.X. Trautwein, J. Phys. Chem. A 101 (1997) 2692–2701.
[49] R. Rutter, L.P. Hager, H. Dhonau, M. Hendrich, M. Valentine, P. Debrunner, Biochemistry 23 (1984) 6809–6816.
[50] R. Rutter, L.P. Hager, J. Biol. Chem. 257 (1982) 7958–7961.
[51] V. Schünemann, F. Lendzian, C. Jung, J. Contzen, A.-L. Barra, S.G. Sligar, A.X. Trautwein, J. Biol. Chem. 279 (2004) 10919–10930.
[52] G. Bleifuß, M. Kolberg, S. Pötsch, W. Hofbauer, R. Bittl, L. Lubitz, A. Gräslund, G. Lassmann, F. Lendzian, Biochemistry 40 (2001) 15362–15368.
[53] A. Ivancich, C. Jakopitsch, M. Auer, S. Un, C. Obinger, J. Am. Chem. Soc. 125 (701) (2003) 14093–14102.
[54] F. Lendzian, Biochim. Biophys. Acta 1707 (2005) 67–90.
[55] A. Ivancich, G. Mazza, A. Desbois, Biochemistry 40 (2001) 6860–6866.
[56] C. Jung, F. Lendzian, V. Schünemann, M. Richter, L.H. Böttger, A.X. Trautwein, J. Contzen, M. Galander, D.K. Ghosh, A.-L. Barra, Magn. Reson. Chem. 43 (2005) 84–95.
[57] C. Jung, V. Schünemann, F. Lendzian, A.X. Trautwein, J. Contzen, M. Galander, L.H. Böttger, M. Richter, A.-L. Barra, Biol. Chem. 386 (10) (2005) 1043–1053.
[58] C. Schulz, R. Rutter, J.T. Sage, P.G. Debrunner, L.P. Hager, Biochemistry 23 (1984) 4743–4754.
[59] C.E. Schulz, P.W. Devaney, H. Winkler, P.G. Debrunner, N. Doan, R. Chiang, R. Rutter, L.P. Hager, FEBS Lett. 103 (1979) 102–105.
[60] M.J. Benecky, J.E. Frew, N. Scowen, P. Jones, B.M. Hoffman, Biochemistry 32 (1993) 11929–11933.
[61] S.H. Kim, R. Perera, L.P. Hager, J.H. Dawson, B.M. Hoffman, J. Am. Chem. Soc. 128 (17) (2006) 5598–5599.
[62] W. Sturhahn, T.S. Toellner, E.E. Alp, X. Zhang, M. Ando, Y. Yoda, S. Kikuta, M. Seto, C.W. Kimball, B. Dabrowski, Phys. Rev. Lett. 74 (1995) 3832–3835.
[63] W. Sturhahn, V.G. Kohn, Hyperfine Interact. 123+124 (2000) 367–399.
[64] H. Paulsen, H. Winkler, A.X. Trautwein, H. Grünsteudel, V. Rusanov, H. Toftlund, Phys. Rev. B 59 (1999) 975–984.
[65] W. Zeng, A. Barabanschikov, Y. Zhang, J. Zhao, W. Sturhahn, E.E. Alp, J.T. Sage, J. Am. Chem. Soc. 130 (2008) 1816–1817.
[66] J.E. Penner-Hahn, K.S. Eble, T.J. McMurry, M. Renner, A. Balch, J.T. Groves, J.H. Dawson, K.O. Hodgson, J. Am. Soc. 108 (1986) 7819–7825.
[67] M.T. Green, J.H. Dawson, H.B. Gray, Science 304 (2004) 1653–1656.
[68] F. van Rantwijk, R.A. Sheldon, Curr. Opin. Biotechnol. 11 (2000) 554–564.
[69] X. He, P.R. Ortiz de Montellano, J. Biol. Chem. 279 (2004) 39479–39484.
[70] S.P. Cramer, J.H. Dawson, K.O. Hodgson, L.P. Hager, J. Am. Chem. Soc. 100 (1978) 7282–7290.
[71] J.E. Hahn, K.O. Hodgson, L.A. Andersson, J.H. Dawson, J. Biol. Chem. 257 (1982) 10934–10941.
[72] N.J. Cosper, R.A. Scott, H. Hori, T. Nishino, T. Iwasaki, J. Biochem. 130 (2001) 191–198.
[73] I. Schlichting, J. Berendzen, K. Chu, A.M. Stock, S.A. Maves, D.E. Benson, R.M. Sweet, D. Ringe, G.A. Petsko, S.G. Sligar, Science 287 (2000) 1615–1622.
[74] V. Fülöp, R.P. Phizackerley, S.M. Soltis, I.J. Clifton, S. Wakazuki, J. Erman, J. Hajdu, S.L. Edwards, Structure 2 (1994) 201–208.
[75] P. Gouet, H.-M. Jouve, P.A. Williams, I. Andersson, P. Andreoletti, L. Nussaume, J. Hajdu, Nat. Struct. Biol. 3 (1996) 951–956.
[76] C. Jung, Leakage in cytochrome P450 reactions in relation to protein structural properties, in: A. Sigel, H. Sigel, R.K.O. Sigel (Eds.), Metal Ions in Life Sciences, The Ubiquitous Roles of Cytochrome P450 Proteins, vol. 3, John Wiley & Sons., Chichester, UK, 2007, pp. 187–234.
[77] C. Jung, Biochim. Biophys. Acta 1814 (2011) 46–57.
[78] R. Weiss, A. Gold, A.X. Trautwein, J. Terner, High-valent iron and manganese complexes of porphyrins and related macrocycles, in: K.M. Kadish, K.M. Smith, R. Guilard (Eds.), The Porphyrin Handbook, vol. 4, Academic Press, Elsevier Science, USA, 2000, pp. 65–96.
[79] K. Jayaraj, A. Gold, R.N. Austin, L.M. Ball, J. Terner, D. Mandon, R. Weiss, J. Fischer, A. DeCian, E. Bill, M. Müther, V. Schünemann, A.X. Trautwein, Inorg. Chem. 20 (1997) 4555–4566.
[80] J.R. Kincaid, Y. Zheng, J. Al-Mustafa, K. Czarnecki, J. Biol. Chem. 271 (1996) 28805–28811.
[81] O. Horner, J.-M. Mouesca, P.L. Solari, M. Orio, J.-L. Oddou, P. Bonville, H.M. Jouve, J. Biol. Inorg. Chem. 12 (2007) 509–525.